

A Theoretical Study of the Decomposition Mechanisms in Substituted *o*-Nitrotoluenes

Guillaume Fayet,^{†,‡} Laurent Joubert,[†] Patricia Rotureau,[‡] and Carlo Adamo^{†,*}

Laboratoire d'Electrochimie, Chimie des Interfaces et Modélisation pour l'Energie, CNRS UMR-7575, Ecole Nationale Supérieure de Chimie de Paris—Chimie ParisTech, 11 rue P. et M. Curie, F-75231 Paris Cedex 05 France, and Institut National de l'Environnement Industriel et des Risques, (INERIS), Parc Technologique Alata, BP2, 60550 Verneuil-en-Halatte, France

Received: June 25, 2009; Revised Manuscript Received: September 28, 2009

The pathways corresponding to the most energetically favorable decomposition reactions that can be envisaged for *o*-nitrotoluene (and 20 of its derivatives) have been studied, using density functional theory, in order to evaluate the influence of substituents' nature (nitro, methyl, amino, carboxylic acid, and hydroxyl) and position. The first mechanism consists of the direct dissociation (homolysis) of the carbon nitrogen bond ($\text{CH}_3\text{C}_6\text{H}_4\text{NO}_2 = \text{CH}_3\text{C}_6\text{H}_4 + \text{NO}_2$) whereas the second one is a more complex process initiated by C–H alpha attack and leading to the formation of anthranil and water ($\text{C}_6\text{H}_4\text{C}(\text{H})\text{ON} + \text{H}_2\text{O}$). For each compound, the initial step of this last channel is the rate limiting one, the Gibbs activation energy of all systems being very close, that is all in the 40–44 kcal/mol range. More important variations have been observed for the C–NO₂ homolysis Gibbs activation energies (46–60 kcal/mol). These variations have been related to electron donor–acceptor properties of substituents by considering significant correlations ($R^2 > 0.9$) with the Hammett parameters (σ). Nevertheless, though the influence of substituents on the direct breaking of the C–NO₂ bond was important, the C–H alpha attack remained finally the major decomposition channel for the studied compounds. Our study underlines the complexity of the decomposition process in nitroaromatic compounds and casts some doubts on the characterization of the energetic properties of such molecules only on the basis of C–NO₂ homolysis.

1. Introduction

Understanding and predicting the decomposition behaviors of energetic materials are very important not only for their physicochemical characterization but also to face the safety problems concerning their use and storage. Many accidents, particularly in chemical processes, have been caused by the lack of knowledge of chemical properties and reactivity.^{1,2} Thus, regulatory initiatives promote the development of efficient tools for better risk management³ and different approaches have been applied to analyze and predict chemical hazards.^{4–8} Commonly, these existing predictive tools are mostly based on empirical rules. However, decomposition mechanisms are intimately connected to the explosive properties of energetic materials, so that any approach giving access to detailed mechanisms of their decomposition could provide significant improvement in chemical hazard prevention. In this sense theoretical chemistry opens new perspectives,^{9–16} not only allowing calculation of thermochemical data¹⁷ but also giving important information on the search for efficient predictive models for other properties of hazardous chemicals, such as thermal^{18,19} or mechanical sensitivities.²⁰ As a matter of fact, explosive properties evaluation is nowadays based on empirical considerations.^{21–23} Moreover, experimental data are not always available or reliable, since experimental conditions and protocols strongly affect the measured properties.²⁴

Nitroaromatic compounds and particularly nitrotoluene derivatives, such as the well-known 2,4,6-trinitrotoluene (TNT), are often considered as prototypical energetic molecules for their

explosive properties²⁵ so that they have been deeply investigated.^{26–30} For instance, several experimental^{31–36} and theoretical^{9,13,16} works have been carried out to characterize and rationalize the decomposition channels of the *o*-nitrotoluene derivatives. Among them, three channels, presented in Figure 1, have been considered as potentially competitive in the decomposition process. The first one is the homolytic dissociation of the nitro group. Such a path is of particular importance, since general assumption in the prediction of explosibility properties considered that the cleavage of the weakest bond, C–NO₂ in nitroaromatic compounds, is mainly responsible of the heat liberated during the explosion.^{37,38} The second one is initiated by a nitro–nitroso (NO₂ → ONO) rearrangement leading to the loss of a NO radical. These two channels are the principal initiation paths in the thermal or photodissociation of nitrobenzene^{28,39,40} and related compounds in the absence of ortho substituents.^{13,16,34} They have also been experimentally identified for ortho-substituted compounds.^{35,36,41} A third channel, the so-called “C–H alpha attack”, is active if a hydrogen of a substituent in ortho position (e.g., the methyl group in *o*-nitrotoluene) is transferred to the nitro group, giving as final products anthranil derivative and water. Such a mechanism has been recognized experimentally as the primary decomposition channel of 2,4,6-trinitrotoluene^{42,43} and 2-nitrotoluene.³¹ It was also proposed for the decomposition of the anion radicals of these compounds⁴⁴ and to explain the decomposition process of generic ortho-substituted nitroaromatic compounds.^{33,34,45} Theoretical studies on TNT, 2,4-dinitrotoluene, and *o*-nitrotoluene lead to similar conclusions.^{9,13,16,46,47}

In the early 1990s, Grever has underlined the importance of the chemical structure on the decomposition of para-substituted nitrobenzenes,²³ and his remarks were later confirmed by Brill.²⁶

* Corresponding author, carlo-adamo@enscp.fr.

[†] ENSCP.

[‡] INERIS.

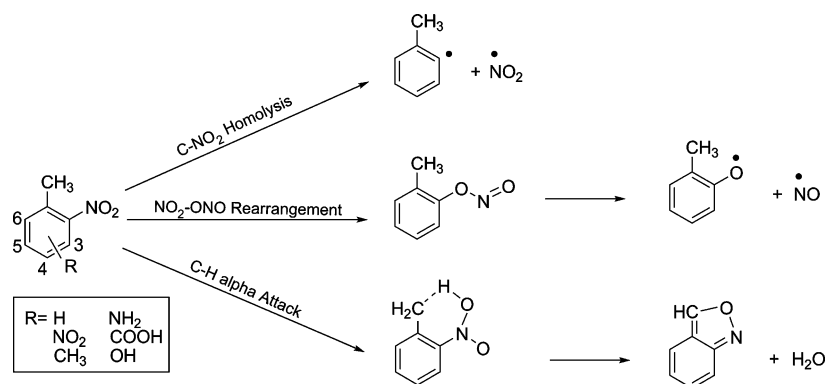


Figure 1. Decomposition channels of the substituted *o*-nitrotoluenes and related atom labeling.

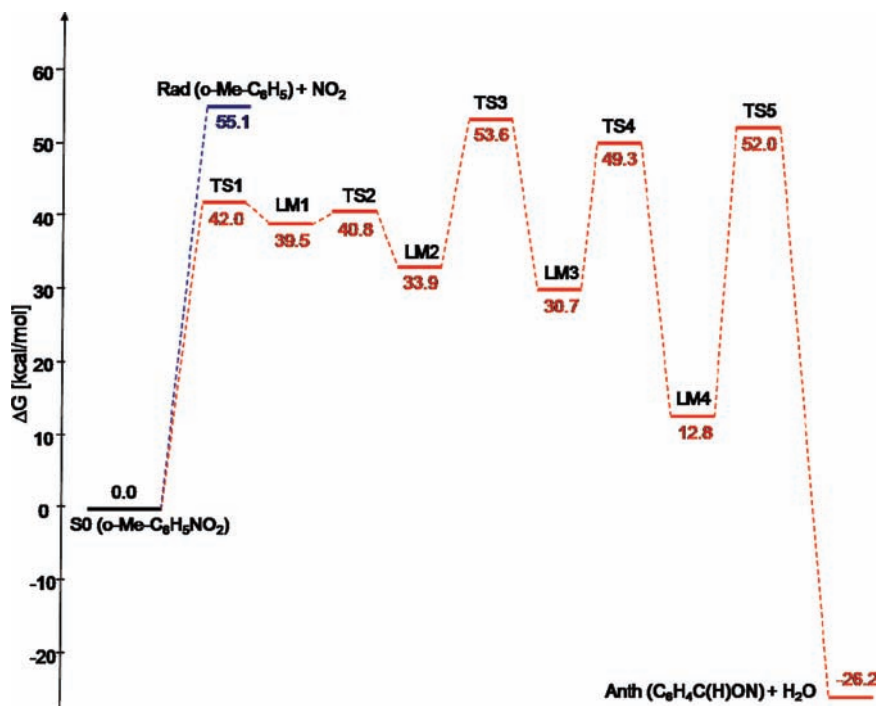


Figure 2. Relative Gibbs free energy diagram for the major decomposition paths of *o*-nitrotoluene calculated at the PBE0/6-31+G(d,p) level: C–NO₂ homolysis (in blue) and C–H alpha attack (in red).

We have recently shown that this could be not the case for a series of substituted nitrobenzenes, where no influence of substituents was observed on the competition between the C–NO₂ bond cleavage and the NO₂–ONO rearrangement, the first channel being always the most energetically favorable.⁴⁸ However no study has been carried out, to the best of our knowledge, concerning the competition between the C–NO₂ bond cleavage and the C–H alpha attack, the two major decomposition paths in substituted *o*-nitrotoluenes. In order to fill this lack, these two reaction paths have been studied, using a theoretical model based on density functional theory (DFT), in *o*-nitrotoluene and 20 derivatives. The latter are obtained by varying the substituent nature (nitro, methyl, amino, carboxylic acid, or hydroxyl groups) and position on the benzyl ring (positions 3, 4, 5, and 6, see Figure 1).

2. Computational Details

All calculations have been carried out using the density functional theory (DFT) with the parameter-free PBE0 hybrid functional⁴⁹ as implemented in the Gaussian03 package.⁵⁰ All the structures of the investigated nitrotoluene derivatives, their decomposition products, local minimum intermediates (LMs),

TABLE 1: Relative Energies (ΔE), Enthalpies (ΔH), and Gibbs Free Energies (ΔG) in kcal/mol for the Two Major Decomposition Channels of *o*-Nitrotoluene at PBE0/6-31+G(d,p)^a

	ΔE		ΔH PBE0	ΔG PBE0
	PBE0	G2M ^b		
S0	0.0	0.0	0.0	0.0
Rad + NO₂	68.7	76.3	69.9	55.1
TS1	40.5	46.3	41.1	42.0
LM1	39.0	37.9	39.6	39.5
TS2	40.2	38.8	40.8	40.8
LM2	33.6	31.9	34.2	33.9
TS3	53.9	52.9	53.5	53.6
LM3	30.4	28.5	31.0	30.7
TS4	47.9	46.1	48.5	49.3
LM4	11.4	11.1	12.0	12.8
TS5	50.6	48.8	51.2	52.0
Anth + H₂O	-17.1	-6.0	-15.9	-26.2

^a See nomenclature in Figure 3. ^b From ref 16, G2M(RCC,MP2)//B3LYP/6-311G(d,p) level.

and transition states (TSs) were computed using a 6-31+G(d,p) basis set. The nature of the stationary points was checked by

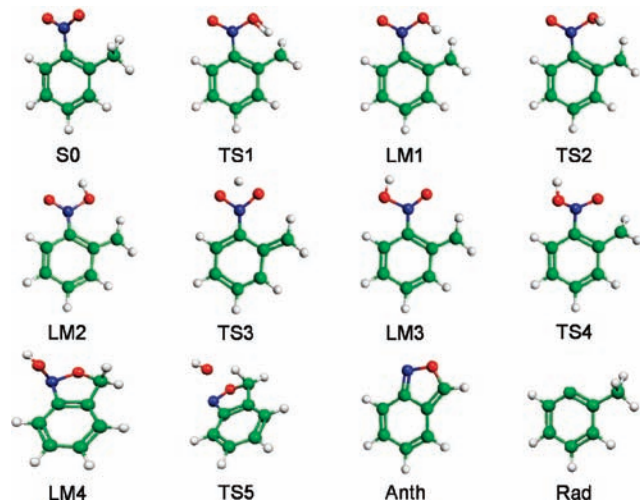


Figure 3. Structures of the different stationary points (minima and transition states) of the major decomposition channels of *o*-nitrotoluene presented in Figure 2.

TABLE 2: Atomic Charge (e^-) of the NO_2 Group Computed from a Natural Population Analysis^a

	carbon 3	carbon 4	carbon 5	carbon 6
-H	-0.26	-0.26	-0.26	-0.26
-NO ₂	-0.17	-0.24	-0.24	-0.23
-CH ₃	-0.24	-0.27	-0.27	-0.25
-NH ₂	-0.31	-0.27	-0.31	-0.25
-COOH	-0.20	-0.25	-0.25	-0.24
-OH	-0.30	-0.27	-0.29	-0.25

^a See Figure 1 for atom numbering.

computing harmonic frequencies. Thermal corrections, enthalpies, and Gibbs free energies were computed from harmonic frequencies using the standard statistical approaches, as implemented in Gaussian03 software,⁵⁰ and natural population analyses (NPA)⁵¹ were performed to describe the electronic structure of these investigated molecules.

Open shell molecules were computed using the spin-unrestricted formalism, and spin contamination appeared neg-

ligible, the obtained values of S^2 being always close to 0.75 for all radical species involved.

3. Results and Discussion

3.1. Reference Reaction: *o*-Nitrotoluene Decomposition.

Free energy profiles of the two investigated decomposition channels of *o*-nitrotoluene are presented in Figure 2, while the corresponding relative energies, enthalpies, and Gibbs free enthalpies are collected in Table 1. The optimized structures of the LMs and TSs along these paths are represented in Figure 3, and the main optimized structural parameters are collected in the Supporting Information. We recall that in a previous study⁴⁸ we have shown that the nitro/nitroso isomerization is not a competitive reaction, the corresponding transition state being at least 5 kcal/mol higher in energy than that of both mechanisms here investigated. Therefore this path will not be considered in the following.

The direct breaking of the C–N bond leads to the formation of the methylphenoxyl ($\text{CH}_3\text{C}_6\text{H}_5$) and nitro (NO_2) radicals. In the second channel, the C–H alpha attack, a hydrogen atom of the methyl group is transferred to the nitro group in the ortho position through **TS1**. The obtained molecule (**LM1**) isomerizes from this “HONO” conformation to a “ONOH” one (**LM3**) in two steps, rotation (**LM2**) and internal hydrogen transfer. Then the most accessible “ONOH” oxygen links to the CH_2 group (**LM4**). Finally, anthranil ($\text{C}_6\text{H}_4\text{CHON}$) and water are formed by the concerted dissociations of C–H and N–OH bonds through **TS5**. All these steps are endothermic even if the final products (anthranil and water) are more stable than the reactants by about 26 kcal/mol.

According to Table 1, the rate-limiting step of the C–H alpha attack channel is the initial one when a hydrogen atom is transferred from the methyl to the nitro group (42.0 kcal/mol). Its activation energy is computed to be significantly lower in energy than the C–NO₂ bond cleavage (55.1 kcal/mol). If this last result is in contradiction with the paradigm considering the C–NO₂ dissociation as the main initiation step for the heat release during an explosion,^{37,38} it is consistent with previous studies considering this reaction path as the major decomposition path of 2-nitrotoluene¹⁶ but also of 2,4,6-trinitrotoluene.¹³ Also

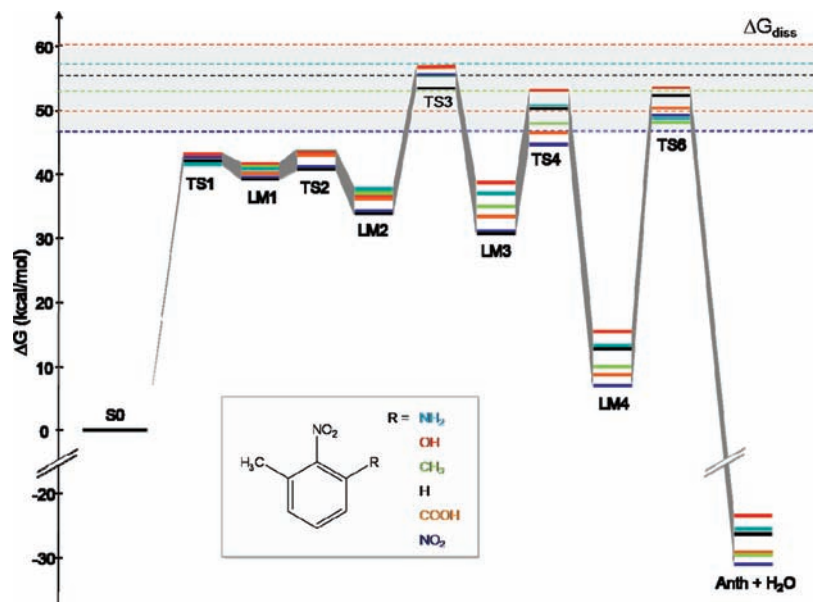


Figure 4. Relative Gibbs free energy diagram for dissociation reactions to H_2O and NO_2 of *o*-nitrotoluenes derivatives substituted on carbon 3 calculated at the PBE0/6-31+G(d,p) level.

TABLE 3: Relative Gibbs Free Energies (kcal/mol) for the Dissociation Reactions to H₂O and NO₂ of *o*-Nitrotoluene and Derivatives Calculated at PBE0/6-31+G(d,p) Level (see Figure 1 for Atom Numbering)

	-H	-NO ₂	-CH ₃	-NH ₂	-COOH	-OH
On Carbon 3						
S0	0.0	0.0	0.0	0.0	0.0	0.0
Rad + NO₂	55.1	46.6	52.4	57.1	49.6	59.6
TS1	42.0	42.6	43.1	41.6	42.5	43.2
LM1	39.5	39.6	41.3	40.7	40.0	41.5
TS2	40.8	41.3	43.5	43.5	42.7	42.9
LM2	33.9	34.3	37.1	37.5	36.0	36.2
TS3	53.6	55.3	55.2	56.3	56.4	56.7
LM3	30.7	31.1	34.5	37.6	32.9	38.3
TS4	49.3	44.3	47.7	50.4	46.1	52.6
LM4	12.8	7.2	9.8	13.1	8.5	15.7
TS5	52.0	49.1	48.0	48.2	50.0	53.4
Anth + H₂O	-26.2	-31.1	-29.6	-25.6	-29.2	-23.6
On Carbon 4						
S0	0.0	0.0	0.0	0.0	0.0	0.0
TS1	42.0	40.7	42.6	42.5	41.1	43.6
LM1	39.5	37.7	39.9	38.8	38.5	38.8
TS2	40.8	39.2	40.9	39.0	39.5	40.9
LM2	33.9	31.8	34.1	32.2	33.1	32.3
TS3	53.6	52.7	53.5	51.2	53.4	53.2
LM3	30.7	28.4	31.0	29.4	29.6	30.7
TS4	49.3	47.7	49.8	48.7	48.3	49.4
LM4	12.8	11.0	13.1	13.4	11.9	13.3
TS5	52.0	51.9	52.6	52.1	52.1	52.9
Anth + H₂O	-26.2	-27.0	-25.6	-28.2	-26.1	-26.2
Rad + NO₂	55.1	52.3	55.4	55.8	53.4	55.2
On Carbon 5						
S0	0.0	0.0	0.0	0.0	0.0	0.0
Rad + NO₂	55.1	52.6	58.9	60.0	53.6	58.9
TS1	42.0	41.9	43.4	41.5	42.2	43.1
LM1	39.5	38.2	41.2	41.0	38.8	41.8
TS2	40.8	38.8	42.7	43.4	39.6	43.8
LM2	33.9	31.2	35.8	36.9	32.4	37.1
TS3	53.6	51.6	55.5	56.5	52.0	56.9
LM3	30.7	28.0	32.8	34.0	28.9	37.1
TS4	49.3	46.7	51.7	52.9	47.8	52.6
LM4	12.8	10.3	15.1	16.5	11.2	15.8
TS5	52.0	51.8	53.4	51.4	51.9	53.0
Anth + H₂O	-26.2	-28.3	-23.7	-22.4	-27.6	-22.6
On Carbon 6						
S0	0.0	0.0	0.0	0.0	0.0	0.0
Rad + NO₂	55.1	50.8	54.4	54.5	52.1	54.1
TS1	42.0	40.5	40.8	41.4	40.2	41.8
LM1	39.5	37.0	38.4	39.7	36.7	37.9
TS2	40.8	39.2	40.2	40.0	39.2	39.9
LM2	33.9	32.8	33.3	33.5	32.8	33.2
TS3	53.6	52.8	52.4	52.4	51.3	51.9
LM3	30.7	29.5	29.8	29.9	29.0	29.3
TS4	49.3	45.6	47.7	47.2	45.8	47.8
LM4	12.8	5.7	10.3	11.4	6.5	11.4
TS5	52.0	46.5	49.4	50.7	46.4	51.4
Anth + H₂O	-26.2	-33.0	-29.0	-28.3	-32.6	-28.0

the energy of **TS2** is lower in energy than the direct C–NO₂ bond cleavage (40.8 kcal/mol), but this latter reaction, the cleavage, is only slightly higher in energy than the TS for the HONO to ONOH isomerization (**LM2** → **LM3** step, 53.6 kcal/mol see Figure 2).

From a computational point of view, it must be pointed out that the relative energies (ΔE) obtained at a PBE0/6-31+G(d,p) level (including vibrational zero-point energies) are close to those obtained by a refined post-Hartree–Fock (G2M) method.¹⁶ Few deviations can be however found, the most striking one being the C–NO₂ dissociation energy (68.7 vs 76.3 kcal/mol). However the PBE0 calculated dissociation enthalpy (69.9 kcal/mol) is in excellent agreement with the experimental value (70.2 ± 2.5 kcal/mol),³⁵ thus supporting the quality of our computational protocol as it was already observed for nitrobenzene.⁴⁸

Finally, due to the relevant entropic effects (e.g., 13.6 kcal/mol on the C–NO₂ dissociation) only Gibbs free energies will be considered in the following.

3.2. Influence of Substituents on Carbon 3. The effect of substituting the initial *o*-nitrotoluene on carbon 3 has been investigated for the five functional groups: nitro, methyl, amino, carboxylic acid, and hydroxyl (–NO₂, –CH₃, –NH₂, –COOH, –OH). In this position, electron donor or acceptor effects are in general difficult to interpret because both electronic and steric effects can play a comparable role due to the spatial vicinity of the nitro and the substituent in position 3. Here, geometric structures (in Table S1 in Supporting Information) and NO₂ charges (Table 2) are influenced by the nature of substituents. The most important changes concern the dihedral angle along the carbon nitrogen bond due, on the one hand, to steric hindrance and, on the other hand, to possible stabilizing interactions (e.g., between the hydrogen of an hydroxyl substituent and an oxygen of the nitro group). Some other geometric parameters seem to follow expectable trends. For instance, the carbon nitrogen bond is shorter (and the nitro charge lower) for electron-donating groups (e.g., 1.44 Å and –0.31 for NH₂) than for electron attracting ones (e.g., 1.47 Å and –0.17 for NO₂, 1.47 Å and –0.20 for COOH). Accordingly, nitro dissociations are more energetic for NH₂ (57.1 kcal/mol) than for NO₂ (46.6 kcal/mol) or COOH (49.6 kcal/mol) as shown in Figure 4 (see Table 3 for energetic values).

Concerning the energies, substitution in position 3 clearly decreases the C–NO₂ bond energy when the group is electron attractor (NO₂, COOH) and increases for electron donors (NH₂ and OH).

For the second decomposition channel, some differences in Gibbs free energies appear when changing the substituent. These variations concern the last steps of the channel (in particular the final products) but not the rate-limiting step. For instance, relative Gibbs free energies range from –31.1 to –23.6 kcal/mol for the final products whereas **TS1** energies remain between 41.6 and 43.2 kcal/mol. A small variation is found instead for **TS3**, whose energy increases of about 2 kcal/mol in all 3-substituted *o*-nitrotoluenes. However, this transition state is generally higher in energy than C–NO₂ bond cleavage energy, except for the amino derivative.

3.3. Influence of Substituents on Carbon 4. In Figure 5 are presented the energetic profiles of the decomposition channels for the five *o*-nitrotoluene derivatives substituted on carbon 4. Corresponding energetic values are reported in Table 3, while the structures are reported in Table S2 in Supporting Information.

As expected, substituent effects on the geometric and electronic structures are less important than those on carbon 3. For example, nitro charge increases only from –0.27 to –0.24 when changing the electron-donating NH₂ for an electron-attracting NO₂ and the C–NO₂ length ranges only 0.004 Å. Indeed, no significant substituent effect is exhibited for the C–H alpha attack which remains the most favorable decomposition channel, all initial hydrogen transfer ΔG values being close to 42 kcal/mol. Small variations, with respect to the unsubstituted toluene, are also observed for the following steps of the channel.

Variations in C–NO₂ dissociation Gibbs free energies are also small (from 52.3 kcal/mol for NO₂ to 55.8 kcal/mol for NH₂). The small observed variations may be due to the fact that the nitro group presents a mesomeric effect in the ortho (carbon 3) and para (carbon 5) positions but not in the meta (carbons 4 and 6, see Figure 6). As a consequence, the rate-

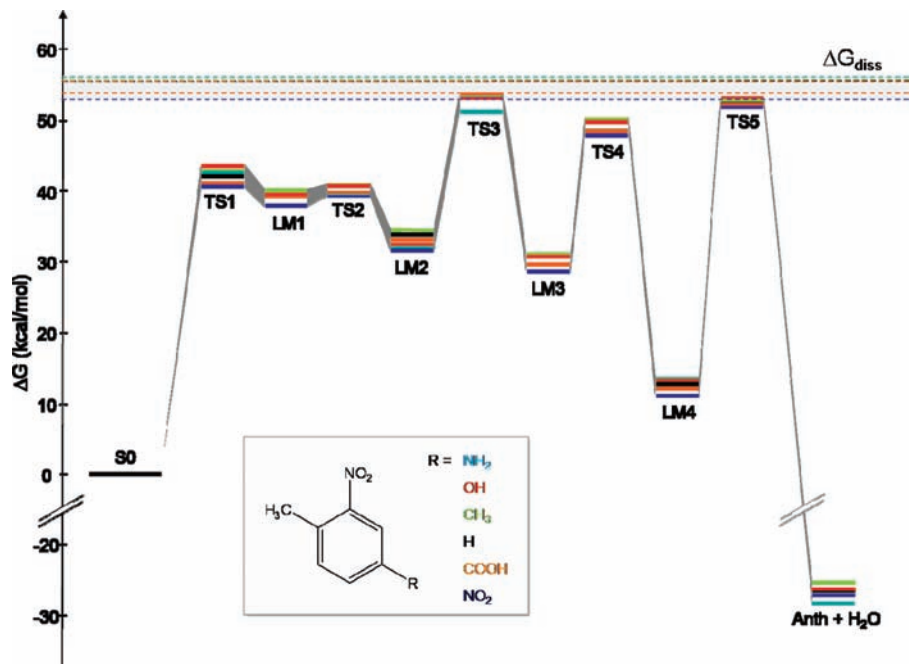


Figure 5. Relative Gibbs free energy diagram for dissociation reactions to H₂O and NO₂ of *o*-nitrotoluenes derivatives substituted on carbon 4 calculated at the PBE0/6-31+G(d,p) level.

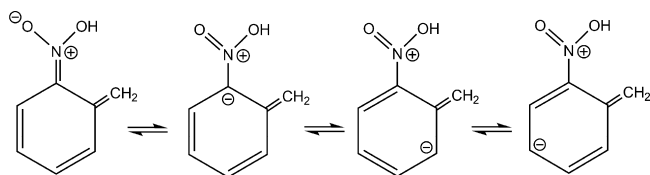


Figure 6. Sketches of the resonance electronic structures for the aci-nitro tautomer of 2-nitrotoluene (LM1).

TABLE 4: Experimental Hammett Constants in Meta and Para Positions (σ_m and σ_p , Respectively) from Reference 49

	σ_m	σ_p
-H	0.00	0.00
-NO ₂	0.71	0.78
-CH ₃	-0.07	-0.17
-NH ₂	-0.16	-0.66
-COOH	0.37	0.45
-OH	0.12	-0.37

limiting step remains the same (TS1) whatever the substituent and the C–H alpha attack is less energetic than the homolysis channel.

However such small variations in C–NO₂ energies can be analyzed in terms of the Hammett constant (σ).⁵² This parameter has been widely used to interpret reaction mechanisms and properties of organic compounds⁵³ and Hammett-like equations have been derived with different molecular descriptors.⁵⁴ Electron-withdrawing groups (NO₂), expected to be highly reactive, present positive values of σ whereas electron-donating groups (NH₂), expected to be less reactive, present negative ones. The experimental values for the para and meta positions, taken from ref 55, are collected in Table 4. We recall that the Hammett equation breaks down for ortho substituents, which exert significant “proximity” effects, which may be polar as well as steric in origin. In Figure 7 are plotted the dissociation free energy variations of the C–NO₂ bond as a function of the Hammett parameter. A nice linear variation ($R^2 = 0.96$) is observed for the substituent on carbon 4, whereas the dependence is not so significant for the activation of the C–H alpha

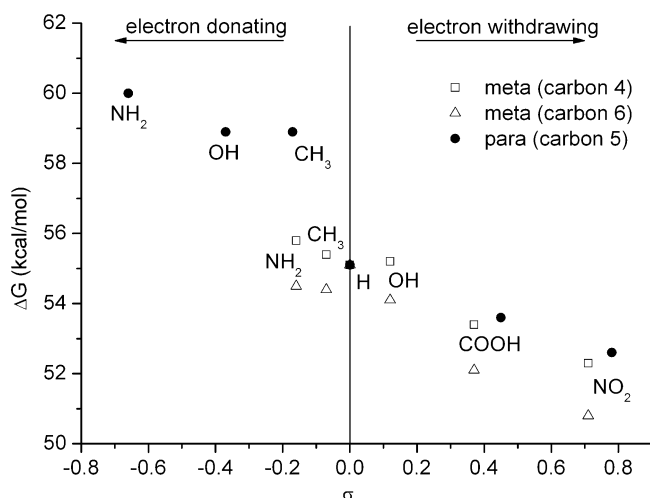


Figure 7. Computed Gibbs free energy variations as a function of the experimental Hammett constant for the dissociation of the C–NO₂ bond for nitrotoluenes substituted on carbons 4, 5, and 6 (see Figure 1 for labeling).

attack channel ($R^2 = 0.71$) or other energies along this channel. Similar breakdown of the Hammett equation has already been observed for activation energies.⁵⁶

3.4. Influence of Substituents on Carbon 5. The structures of *o*-nitrotoluene derivatives with different substituents (nitro, methyl, amino, carboxylic acid, and hydroxyl) on carbon 5 are presented in Table S3 in Supporting Information and total charges on the nitro group are reported in Table 2. As expected, the most electron-donating group (amino) leads to the highest value of charge for the leaving nitro group (−0.24) whereas the most electron-withdrawing one (nitro) leads to the lowest value (−0.31). Geometric structures follow this trend as the carbon–nitrogen distance is maximal for the nitro substituent (1.47 Å) and decreases down to 1.45 Å for amino.

The energies of the different stationary points along the two investigated decomposition channels are reported in Table 3. Carbon 5 substitution has more influence than the carbon 4 due

to mesomeric effect of the nitro group (see Figure 2). The C–NO₂ bond breaking Gibbs free energy ranges from 52.6 (NO₂) to 60.0 kcal/mol (NH₂). Once again, this can be correlated to the electron-donor or -acceptor properties of substituents, considering para Hammett constants ($R^2 = 0.91$) as shown in Figure 7.

No such dependency is observed on the second decomposition channel. If most of the stationary points are influenced by the substituent nature (for instance, reaction products range from –28.3 kcal/mol for NO₂ to –22.4 kcal/mol for NH₂), this is not the case for the first barrier, rate-limiting step of the mechanism (from 41.5 kcal/mol for NO₂ to 43.4 kcal/mol for CH₃). This may be due to a most favorable propagation of electronic effect within the cyclic conformation in anthranyl-like structures than in initial nitrotoluene-like ones. In contrast small variations can be observed for the LM intermediates, which result to be more (less) stable with respect to the reference nitrotoluene derivatives when electron attractor (donor) groups are present in position 5. This behavior can be qualitatively rationalized looking at the resonance structures of the LM1 and LM2 intermediates (see Figure 6): any electron-withdrawing group, stabilizing the negative charge in position 5, increases the stability of the two intermediates. This is not the case for derivatives substituted in positions 4 and 6, whereas for those substituted in position 3. Such a feature is hidden by strong direct (steric and electronic) interactions.

However, whatever the substituent in carbon 5, the competition between the two decomposition channels is the same. C–H alpha attack process is lower in energy than C–NO₂ homolysis.

3.5. Influence of Substituents on Carbon 6. The last investigated position for the substitution is located ortho of the methyl group. The different geometric parameters and NPA charges are reported in Table S4 in Supporting Information and Table 2, respectively.

No significant variation in nitro charge is observed upon the substituent nature: from –0.26 (H) to –0.23 (NO₂). Accordingly, all carbon–nitrogen bonds range only 0.004 Å.

As for substitution on carbon 4, the substitution is in the meta position with the nitro group, which does not present any mesomeric effect in this position. Nevertheless, significant changes in ΔG s appeared in each channel (see Table 3). This can be explained by ortho effects with the close methyl group. For the C–NO₂ homolysis, Gibbs free energies range from 50.8 kcal/mol for NO₂ to 55.1 kcal/mol for H. Moreover they are significantly correlated with meta Hammett constants ($R^2 = 0.91$) in Figure 7.

For the second reaction path, the first part of the process (hydrogen transfer from CH₃ to the furthest oxygen of the nitro group) is not influenced by the substitution whereas the second part, leading to the formation of anthranil, is significantly affected by the substitution as observed for carbon 5 substitution.

Finally, competition between the two decomposition channels is not more influenced in this position than in the three previously considered ones. The C–H alpha attack is energetically favorable with respect to the C–NO₂ bond cleavage.

4. Conclusion

The influence of the substituent nature and position on the decomposition channels of *o*-nitrotoluene derivatives has been studied using the density functional theory. The first channel considered was the direct dissociation of the C–NO₂ bond (CH₃C₆H₄ + NO₂), since this was the most energetically favored path for the related nitrobenzene. The second one consists in the C–H alpha attack leading to the formation of anthranil and

water (C₆H₄C(H)ON + H₂O). Our calculations suggest that indeed this last channel is the lowest in energy for *o*-nitrotoluene.

Both reactions have been also analyzed for 20 derivative compounds obtained by changing the substituent nature (nitro, methyl, amino, carboxylic acid, and hydroxyl) in the four positions, remaining available on the reference *o*-nitrotoluene ring. Influence of substituent on the dissociative mechanism has relied on the corresponding Hammett parameters σ , as descriptors of the electron donor/acceptor properties of substituents.

Again, our results indicate that, whatever the molecule, the C–H alpha attack mechanism appeared the most favorable. Independently on the substituent, the rate-limiting step remained the initial hydrogen transfer from CH₃ to the NO₂ group and no important variation was observed on the corresponding Gibbs free energies (40–44 kcal/mol) contrary to what is observed for the C–NO₂ dissociation (46–60 kcal/mol).

From a more general point of view, our study pointed out the complexity of the decomposition process in nitroaromatic compounds. Furthermore it suggests that, contrary to the commonly accept experimental axiom, the C–NO₂ homolysis is not the predominant path for the studied *o*-nitrotoluene derivatives.

Acknowledgment. G.F., L.J., and C.A. thank INERIS for a financial support. The completion of this paper has been made possible by the invitation of C.A. at the Institute of Mathematics and its Applications, University of Minnesota, within the Thematic Year on “Mathematics and Chemistry”.

Supporting Information Available: A figure showing atom numbering for the 16 calculated stationary points and tables of structural parameters. This material is available free of charge via the Internet at <http://pubs.acs.org>.

References and Notes

- (1) Etchells, J. C. *Org. Process Res. Dev.* **1997**, *1*, 435.
- (2) Gustin, J.-L. *Org. Process Res. Dev.* **1998**, *2*, 27.
- (3) *Lee's Loss Prevention in Process Industries: Hazard Identification, Assessment and Control*, 3rd ed.; Mannan, S., Ed.; Elsevier Butterworth-Heinemann: Burlington, MA, 2005.
- (4) Lewis, A.; Kazantzis, N.; Fishtik, I.; Wilcox, J. *J. Hazard. Mater.* **2007**, *142*, 592.
- (5) Melhem, G. A.; Shanley, E. S. *Process Saf. Prog.* **1996**, *15*, 168.
- (6) Shanley, E. S.; Melhem, G. A. *J. Loss Prev. Process Ind.* **1995**, *8*, 261.
- (7) Yoshida, T. *Safety of Reactive Chemicals*; Elsevier: Amsterdam, 1987; Vol. 1.
- (8) Lothrop, W. C.; Handrick, G. R. *Chem. Rev.* **1949**, *44*, 419.
- (9) Tanaka, G.; Weatherford, C. *Int. J. Quantum Chem.* **2008**, *108*, 2924.
- (10) Korolev, V.; Petukhova, T.; Pivina, T.; Porollo, A.; Sheremetev, A.; Suponitskii, K.; Ivshin, V. *Russ. Chem. Bull. Int. Ed.* **2006**, *55*, 1388.
- (11) Liu, M.-H.; Hong, C. C.; Y, S. *Int. J. Quantum Chem.* **2005**, *102*, 398.
- (12) Xu, S.; Lin, M. C. *J. Phys. Chem. B* **2005**, *109*, 8367.
- (13) Cohen, R.; Zeiri, Y.; Wurzburg, E.; Kosloff, R. *J. Phys. Chem. A* **2007**, *111*, 11074.
- (14) Gindulyte, A.; Massa, L.; Huang, L.; Karle, J. *J. Phys. Chem. A* **1999**, *103*, 11040.
- (15) Gindulyte, A.; Massa, L.; Huang, L.; Karle, J. *J. Phys. Chem. A* **1999**, *103*, 11045.
- (16) Chen, S. C.; Xu, S. C.; Diau, E.; Lin, M. C. *J. Phys. Chem. A* **2006**, *110*, 10130.
- (17) Saraf, S. R.; Rogers, W. J.; Ford, D. M.; Mannan, M. S. *Fluid Phase Equilib.* **2004**, *222–223*, 205.
- (18) Fayet, G.; Rotureau, P.; Joubert, L.; Adamo, C. *J. Hazard. Mater.* **2009**, *171*, 845.
- (19) Fayet, G.; Joubert, L.; Rotureau, P.; Adamo, C. *Chem. Phys. Lett.* **2009**, *467*, 407.
- (20) Rice, B. M.; Hare, J. J. *J. Phys. Chem. A* **2002**, *106*, 1770.
- (21) Shanley, E. S.; Melhem, G. A. *Process Safety Prog.* **1995**, *14*, 29.
- (22) Keshavarz, M. H. *J. Hazard. Mater.* **2007**, *142*, 54.
- (23) Grever, T. *Thermochim. Acta* **1991**, *187*, 133.

- (24) Kersten, R. J. A.; Boers, M. N.; Stork, M. M.; Visser, C. *J. Loss Prev. Process Ind.* **2005**, *18*, 145.
- (25) Medard, L. *Les explosifs occasionnels*; TEC & DOC: Cachan, France, 1987.
- (26) Brill, T. B.; James, K. J.; Chawla, R.; Nicol, G.; Shukla, A.; Futrell, J. H. *J. Phys. Org. Chem.* **1999**, *12*, 819.
- (27) Galloway, D. B.; Bartz, J. A.; Huey, L. G.; Crim, F. F. *J. Chem. Phys.* **1993**, *98*, 2107.
- (28) Galloway, D. B.; Glenewinkelmeyer, T.; Bartz, J. A.; Huey, L. G.; Crim, F. F. *J. Chem. Phys.* **1994**, *100*, 1946.
- (29) McCarthy, E.; O'Brien, K. *J. Org. Chem.* **1980**, *45*, 2086.
- (30) Fields, E.; Meyerson, S. *J. Am. Chem. Soc.* **1967**, *89*, 3224.
- (31) He, Y. Z.; Cui, J. P.; Mallard, W. G.; Tsang, W. *J. Am. Chem. Soc.* **1988**, *110*, 3754.
- (32) Kosmidis, C.; Ledingham, K. W. D.; Kilic, H. S.; McCanny, T.; Singhal, R. P.; Langley, A. J.; Shaikh, W. *J. Phys. Chem. A* **1997**, *101*, 2264.
- (33) Shao, J.-D.; Baer, T. *Int. J. Mass Spectrom. Ion Proc.* **1988**, *86*, 357.
- (34) Brill, T. B.; James, K. J. *Chem. Rev.* **1993**, *93*, 2667.
- (35) Gonzalez, A. C.; Larson, C. W.; McMillen, D. F.; Golden, D. M. *J. Phys. Chem.* **1985**, *89*, 4809.
- (36) Tsang, W.; Robaugh, D.; Mallard, W. G. *J. Phys. Chem.* **1986**, *90*, 5968.
- (37) Theerlynck, E.; Mathieu, D.; Simonetti, P. *Thermochim. Acta* **2005**, *426*, 123.
- (38) Saraf, S. R.; Rogers, W. J.; Mannan, M. S. *Ind. Eng. Chem. Res.* **2003**, *42*, 1341.
- (39) Galloway, D. B.; Bartz, J. A.; Huey, L. G.; Crim, F. F. *J. Chem. Phys.* **1993**, *98*, 2107.
- (40) McCarthy, E.; O'Brien, K. *J. Org. Chem.* **1980**, *45*, 2086.
- (41) Fields, E.; Meyerson, S. *J. Am. Chem. Soc.* **1967**, *89*, 3224.
- (42) Rogers, R. N. *Anal. Chem.* **1967**, *39*, 730.
- (43) Dacons, J. C.; Adolph, H. G.; Kamlet, M. J. *J. Phys. Chem.* **1970**, *74*, 3035.
- (44) Batz, M. L.; Garland, P. M.; Reiter, R. C.; Sanborn, M. D.; Stevenson, C. D. *J. Org. Chem.* **1997**, *62*, 2045.
- (45) Kosmidis, C.; Ledingham, K. W. D.; Kilic, H. S.; McCanny, T.; Singhal, R. P.; Langley, A. J.; Shaikh, W. *J. Phys. Chem. A* **1997**, *101*, 2264.
- (46) Il'ichev, Y. V.; Wirz, J. *J. Phys. Chem. A* **2000**, *104*, 7856.
- (47) Murray, J. S.; Lane, P.; Politzer, P.; Bolduc, P. R.; McKenney, R. L. *J. Mol. Struct.: THEOCHEM* **1990**, *209*, 349.
- (48) Fayet, G.; Joubert, L.; Rotureau, P.; Adamo, C. *J. Phys. Chem. A* **2008**, *112*, 4054.
- (49) Adamo, C.; Barone, V. *J. Chem. Phys.* **1999**, *110*, 6158.
- (50) Frisch, M. J.; Trucks, G. W.; Schlegel, H. B.; Scuseria, G. E.; Robb, M. A.; Cheeseman, J. R.; Montgomery, J. A., Jr.; Vreven, T.; Kudin, K. N.; Burant, J. C.; Millam, J. M.; Iyengar, S. S.; Tomasi, J.; Barone, V.; Mennucci, B.; Cossi, M.; Scalmani, G.; Rega, N.; Petersson, G. A.; Nakatsuji, H.; Hada, M.; Ehara, M.; Toyota, K.; Fukuda, R.; Hasegawa, J.; Ishida, M.; Nakajima, T.; Honda, Y.; Kitao, O.; Nakai, H.; Klene, M.; Li, X.; Knox, J. E.; Hratchian, H. P.; Cross, J. B.; Bakken, V.; Adamo, C.; Jaramillo, J.; Gomperts, R.; Stratmann, R. E.; Yazyev, O.; Austin, A. J.; Cammi, R.; Pomelli, C.; Ochterski, J. W.; Ayala, P. Y.; Morokuma, K.; Voth, G. A.; Salvador, P.; Dannenberg, J. J.; Zakrzewski, V. G.; Dapprich, S.; Daniels, A. D.; Strain, M. C.; Farkas, O.; Malick, D. K.; Rabuck, A. D.; Raghavachari, K.; Foresman, J. B.; Ortiz, J. V.; Cui, Q.; Baboul, A. G.; Clifford, S.; Cioslowski, J.; Stefanov, B. B.; Liu, G.; Liashenko, A.; Piskorz, P.; Komaromi, I.; Martin, R. L.; Fox, D. J.; Keith, T.; Al-Laham, M. A.; Peng, C. Y.; Nanayakkara, A.; Challacombe, M.; Gill, P. M. W.; Johnson, B.; Chen, W.; Wong, M. W.; Gonzalez, C.; Pople, J. A. *Gaussian03*; Gaussian Inc.: Wallingford, CT, 2004.
- (51) Reed, A. E.; Weinhold, F. *J. Chem. Phys.* **1985**, *83*, 1736.
- (52) Hammett, L. P. *J. Am. Chem. Soc.* **1937**, *59*, 96.
- (53) Jacquemin, D.; Champagne, B.; André, J.-M. *Synth. Met.* **1996**, *80*, 205.
- (54) Perez, P.; Simon-Manso, Y.; Aizman, A.; Fuentealba, P.; Contreras, R. *J. Am. Chem. Soc.* **2000**, *122*, 4756.
- (55) Hansch, C.; Leo, A.; Taft, R. W. *Chem. Rev.* **1991**, *91*, 165.
- (56) Palat, K. J.; Böhm, S.; Braunerova, G.; Waissner, K.; Exner, O. *New J. Chem.* **2002**, *26*, 861.

JP905979W